THE FEATURES OF HETEROGENEOUS WATER DROPLET EVAPORATION IN HIGH-TEMPERATURE COMBUSTION PRODUCTS OF TYPICAL FLAMMABLE LIQUIDS

by

Maxim V. PISKUNOV, Pavel A. STRIZHAK*, Roman S. VOLKOV, and Alena O. ZHDANOVA

National Research Tomsk Polytechnic University, Tomsk, Russia

Original scientific paper
https://doi.org/10.2298/TSCI150814008P

This paper presents the experimental results on heating and evaporation features of heterogeneous (with opaque solid particles – the size of 0.05-0.5 mm, relative mass concentration 0-1%) water droplets (the initial size – radius 1-3 mm) during their motion through high-temperature (500-1800 K) gases. A significant increase in the integral characteristics of evaporation by introducing opaque inclusions into droplets was observed. The influence of energy accumulation on the conditions of droplet evaporation at the internal solid/liquid interfaces was established. For proportioned inclusions, the conditions of intensive vaporization (leading to the explosive disintegration of droplets) at internal inclusion/liquid interfaces was set. To summarize research results, experiments were conducted with the combustion products of kerosene, gasoline, industrial alcohol, acetone, and oil. The particles of graphite, carbon, and aluminum as solid inclusions were used. The investigation compared integral characteristics of heterogeneous droplet evaporation under the conditions of non-stationary (gas temperature varied from 1800 K to 500 K over the length of channel) and nearly stationary (gas temperature was maintained at about 1100 K) heating.

Key words: *heterogeneous droplets, water, solid inclusions, evaporation, high-temperature combustion products, flammable liquids*

Introduction

The improvement of the efficiency of many power units and plants is traditionally held by different approaches. The most common are: design changes, choice of optimum technological parameters, variation of raw materials or energy sources, production of complex composite fuels, and development of new technological cycles or upgrading of the existing ones. The most cost-effective approaches are, of course, a selection of the optimum parameters of the technological equipment and changing the component composition of working fluids. One such example is power plants operating with high-temperature gas-vapor-droplet mixtures. As described in [1-5], such installations are used in producing heat carriers based on flue gases, steam, and water droplets; thermal or flame treatment of liquids, suspensions, and emulsions; scrubbing of thermal loaded slagged surfaces of power equipment; defrost of granular media; polydisperse firefighting.

* Corresponding author, e-mail: pavelspa@tpu.ru

It should be noted that in the high-temperature (usually more than 1000 K) gas-vapor-droplet technologies listed in [1-5], the optimal choice of parameters (gas temperature, droplet velocity and sizes, the concentration of vapor, droplets, and gases) provides a high efficiency of facilities, despite the fact that a substantial source is required to generate high-temperature gas. In particular, it becomes possible to complete the evaporation of droplets with specified sizes for short periods of time (from several seconds to tens of milliseconds). In industries, such parameters are determined mostly empirically. This is due to the complexity of their control under the conditions of intensive phase transitions (*e. g.*, during the evaporation of water droplets with the size of less than 1 mm in the flow of combustion products or air with a temperature of more than 1000 K). It is particularly difficult to monitor the sizes of heterogeneous droplets (with various impurities and inclusions). In this case, upon intensive phase transitions, a significant transformation of a droplet surface during heating is possible.

To date, very few research results are known about the evaporation of water droplets, suspensions, and water-based emulsions, in gases with temperatures more than 1000 K. There are empirical data [6-8] for homogeneous water droplets (without additional impurities and inclusions). However, they are only valid within a rather limited temperature range (generally less than 500 K) [9]. Moreover, they do not take into account defining processes at the droplet/gas interface, such as radiative heat transfer, energy consumption for heating the emerging water vapor. It is traditionally considered [6-8] that all heat supplied to a droplet is expended on its evaporation. Numerical studies [9, 10] demonstrated that at gas temperatures more than 1000 K, the empirical values of evaporation rates, established using the approach described in references [6-8], differ significantly (by several times) from those found in the experiments of papers [11-13]. Theoretical models [9, 10] allowed us to obtain satisfactory correspondence to the experimental results of studies [11-13] by taking into account almost a full range of heat and mass transfer processes near the droplet/gas interface.

For heterogeneous droplets (with additional impurities and inclusions), such studies were performed only for a limited gas temperature range (1100 ± 30 K) [13]. We can assume that such heating conditions are almost stationary. It is possible to develop the models of such droplet evaporation taking into account a full range of defining effects and processes. This can be performed by experimental investigations for a group of typical combustion products with a change of their temperature in a fairly wide range (from 300-400 K to the maximum possible several thousand degrees). That is, it is important to study the characteristics of heterogeneous droplet evaporation under the conditions of stationary and non-stationary heating typical of modern gas-vapor-droplet heat technologies (for example, considered in reports [1-5]). To summarize the data of experiments [13], it is appropriate to vary the droplet size, as well as the type, size, and concentration of inclusions, in the same ranges as in papers [11-13]. We should consider typical liquid petroleum products (fuel and flammable liquids) as liquid combustibles. This is due to their widespread use as basic combustible substances for the formation of combustion products in high-temperature heat technologies.

The aim of this paper is to investigate experimentally the evaporation features of suspension droplets based on water and opaque solid particles in the high-temperature combustion products of typical flammable liquids.

Experimental set-up and methods

In our experimental studies, we used a set-up, which is depicted in the photo of fig. 1. The facility was equipped with the following photo and video recording tools: CCD video cameras IMPERX IGV B2020M, high-speed CMOS video cameras Phantom V411 and

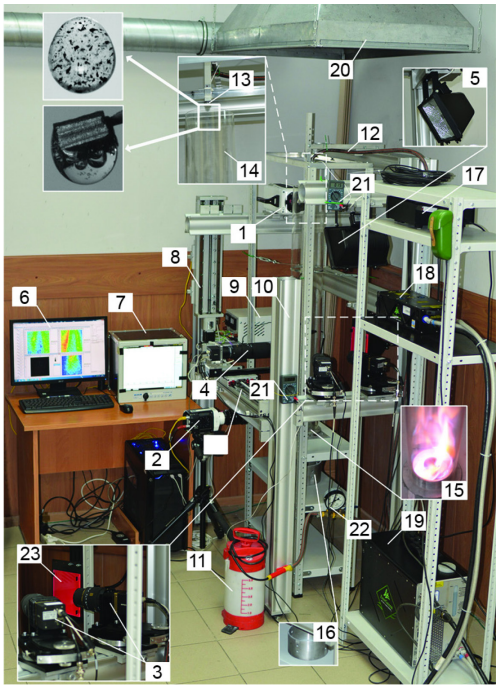

Figure 1. Experimental set-up; *1, 2 – high-speed video cameras, 3, 4 – cross-correlation cameras, 5 – spotlight, 6 – personal computer, 7 – multichannel registrar, 8 – motorized positioning device, 9 – power supply for motorized device, 10 – aluminum rack, 11 – container with a suspension, 12 – suspension supply channel, 13 – dosing device, 14 – quartz tube, 15 – hollow cylinder with a flammable liquid, 16 – water catcher, 17 – synchronizer for a computer, cross-correlation camera, and laser, 18 – solid double-pulse laser, 19 – laser line generator, 20 – air flow system, 21 – digital temperature meter, 22 – manometer, 23 – diffusion screen*

Phantom MIRO M310. For processing the video of experiments, we used Tema Automotive software [14], as well as actual flow with panoramic optical techniques shadow photography (SP) [15], interferometric particle imaging [16], particle tracking velocimetry (PTV) [17], and particle image velocimetry (PIV) [18]. For this purpose, the set-up had an illumination system (similar to that used in studies [11, 12]) based on a double pulsed Nd:YAG laser 18. In the set with the laser 18, a diffuse screen 23 was mounted on the set-up, for illuminating droplets, in order to record them applying the SP method [15].

To generate the high-temperature gas flow, we used a set of devices, consisting of a hollow cylinder 14 (material-quartz) and an aluminum burner 15. Before the experiments, the burner 15 was filled with a flammable liquid, which was then ignited. The tube 14 was mounted on the burner 15 via special grooves. After 200 seconds, the inner cavity of the cylinder 14 was heated up to stable temperatures (deviations not exceed 15-20 K). This was followed by the release of droplets to the zone of high-temperature combustion products and their photo and video recording.

We used the typical flammable liquids for high-temperature gas generation: gasoline (92 octane), kerosene (type TS-1), technical acetone (dimethyl ketone), industrial alcohol (synthetic ethyl), low-grade oil (density ρ = 847 kg/m^3, East Urengoy field, Tyumen Region, Russian Federation). A flue gas temperature T_g was monitored over the entire height of the cylinder 14 at its axis of symmetry using type C thermocouples (temperature measurement range 0-2473 K, permissible error $\pm 0.005|T_g|$), similar to the experiments described in reports [11, 12]. In our experiments, the values of T_g varied from 500 K to 1800 K over the height of the tube 14. The values of T_g in the cylinder 14 for the combustion products are shown in tab. 1. Thus, a droplet was evaporated as it was falling in the channel 14 under non-stationary conditions corresponding to typical high-temperature gas-vapor droplet heat technologies (for example, discussed in references [1-5]). In the experiments of studies [11, 12], the temperature

Table 1. Flue gas temperature (T_g ± 15 K) in the cylinder 14 for considered combustible liquids

The position of thermocouple relative to the base of tube, [m]	0.1	0.3	0.5	0.7	1
Kerosene	1581	1073	802	678	572
Industrial ethanol	1522	978	716	593	505
Gasoline	1790	1211	904	758	632
Acetone	1694	1113	825	721	595
Oil	1280	925	691	570	500

of combustion products T_g was maintained at about 1100 K throughout the length of the tube 14 (the droplet moved under nearly stationary heating conditions).

We used a suspension based on water with an admixture of solid opaque particles in order to generate droplets as liquids under study. We used particles (material: carbon, graphite, aluminum) with sizes L_p = 0.05-0.5 mm; their relative mass concentration in the suspension was 0-1%. We took the maximum linear length of the particle (regardless of its actual shape) as the size (L_p) of an inclusion (a particle). Inclusions (particles) had the shapes of an irregular polyhedron.

A suspension based on water and opaque particles in a container 11 was prepared. For this purpose, we put particles with certain sizes, which we previously prepared, to the cylinder 11 in the desired amount. In order to prevent the sedimentation of particles in the suspension, the suspension was continuously stirred throughout generating droplets in the experiments (with the help of a motorized paddle device embedded in the base of the container 11).

The initial suspension temperature T_w (near 300 K) was monitored in two points by digital temperature meters 21 (directly in the container 11 and at the input of the dosing device 13) with type L thermocouples (temperature measurement range 273-473 K, systematic error ±1.5 K).

The following droplets from the suspension were generated. The suspension prepared in the container 11 was fed to the input of the dosing device 13 through channel 12. The necessary parameters of droplet release in the dosing device 13 (size R_d, the initial velocity U_d, and feed rate) was set. In our experiments, the initial size R_d varied from 1 mm to 3 mm. The initial droplet velocities U_d varied from 0.5 to 2 m/s. Suspension droplets were falling along the symmetry axis of the cylinder 14; thus, they passed the distance of 1 m in high-temperature combustion products.

The mass concentration of inclusions in a droplet immediately before the ignition of a combustible liquid in the burner 15 was determined. Several generated suspension droplets (usually 2-4) were sequentially put on the laboratory microbalance VIBRA AF 225DRCE (in increments of 0.00001 g). Thus, the mass of each droplet m_d with solid inclusions could be found. After that, the time until complete evaporation of water was recorded. Authors were interested in the time interval, when the mass of the suspension placed on the weighing system did not change (its change did not exceed the measurement error). The mass of solid inclusions m_p was measured. Then, the mass concentration of impurities in a droplet was determined: $\gamma_p = m_p/m_d$. The experiments were carried out at γ_p = 0-0.01.

Cameras 1 and 2 recorded images of moving droplets. This approach allowed to calculate the integral parameters of evaporation for each droplet by subsequent comparison of videograms. Droplet sizes were defined from videograms as follows. Four maximum diameters (in pixels) of each suspension droplet were determined using Phantom Camera Control (PCC) software. Then the diameter was averaged: $d_1 = (d_{01} + d_{02} + d_{03} + d_{04})/4$. After calculating the average size of each droplet, an average diameter of all droplets was found: $d_{drop(px)} = (d_1 + d_2 +$

$+\ldots+ d_n)/n$. After that, by knowing a scale factor S (mm/px) found in the step of measuring system calibration, authors converted the diameter to millimeters: $d_{drop(mm)} = d_{drop(px)} \times S$. Finally, the appropriate values of the average droplet radius were calculated.

Similarly, droplet velocities were found. For this purpose, in videogram, authors indicated the point with droplet coordinates at the initial time (when it appeared in the frame) using PCC software. Then, droplet coordinates at the end of the frame was determined. Investigation defined the time of droplet motion between these two points t_d and the distance passed by the droplet in pixels, $l_{d(px)}$. After that, the average droplet velocity (in pixels) was calculated: $U_{d(px/s)} = l_{d(px)}/t_d$. At a certain scale factor S (mm/px), authors converted the velocity to absolute units: $U_d = U_{d(px/s)} \times S$, m/s. Errors in determining sizes and distances using this approach did not exceed 1 px (*i. e.*, in the experiments 0.01-0.02 mm).

Videograms were also processed using Tema Automotive software when determining sizes R_d and velocities U_d. Video processing by Correlation and Circular Symmetry algorithms [14] allowed to visualize each droplet trajectory in the observed area and calculate velocity U_d. By applying Airbag and Advanced Airbag tracking algorithms, the change in the shapes of droplets during their motion was monitored. The values of droplet cross-sectional areas were determined and, as a consequence, the average radius R_d was calculated. This approach made it possible to further clarify the values of R_d. With the use of Tema [14], systematic errors in measuring droplet sizes did not exceed 0.025 mm, the times of their falling – $2 \cdot 10^{-4}$ seconds. The maximum errors in determining droplet velocities were 0.05 m per second.

The SP method [15] for the additional measurement of droplet sizes R_d at the output of the high-temperature gas zone was applied. For that, a diffuse screen 24 was placed directly behind moving droplets at the output of the cylinder 14. The screen was connected to a laser 18 via an optical fiber. In order to ensure laser illumination with the required parameters (intensity, the scattering angle) for droplets, special diffusers (lenses) were installed at the connection point of the optical fiber to the screen. Thus, a diffuse light source was formed with uniform spatial intensity distribution. Authors configured the power of each laser modulator 18 to obtain a satisfactory contrast of droplet shadow images. The focal length of the CCD camera was in close proximity to the object of study for the highest definition of the shadow image. Therefore, it was implemented the backlighting of droplet trajectories and recording of this process by the CCD camera. The subsequent digital analysis of the shadow image allowed us to determine droplet position, border, and size. Also, we applied median, low pass, and average software filters to reduce noise in captured images using Laplace edge detection procedure we indicated droplet borders. When calculating droplet sizes, we applied the Bubbles identification algorithm. The error in determining R_d by the SP method did not exceed 0.3%.

The PTV method was applied [17] to determine droplet velocities. This method is based on measuring the velocity of each particle (droplet) in the observed area. By using SP and PTV methods, we could find simultaneously each droplet size and velocity in the observed area (without overlapping series of experiments). As a consequence, the maximum errors in determining U_d were 0.03 m/s.

The velocity of the high-temperature gas flow U_g was controlled by a system *20* in a narrow range of about 1.5 m/s. Authors measured U_g using the PIV method [18]. Before the release of suspension droplets to the tube 14, we introduced the tracer particles of TiO_2 powder (particles with sizes about 100 nm) to its bottom part. Tracers were blown up by the upward flow of combustion products in the cylinder 14. A laser line 18 was directed to the flow

of high-temperature combustion products. At the same time, we started the photo recording procedure of the process under study by the cross-correlation CCD camera 3. Velocity fields of combustion products were drawn on the displacements of tracer particles, and then the average velocities U_g were found. The procedures of image processing were similar to that described in references [11, 12]. Errors in determining U_g did not exceed 3%.

Authors took the ΔR parameter as an integral parameter of the motion of heterogeneous droplets through high-temperature gases (as in studies [11, 12]): $\Delta R = (R_d - R_d^*)/R_d$; R_d and R_d^* [mm] – droplet radius at the input and output from high-temperature gases. Measured R_d and U_d parameters at the input and output of the tube 14 were measured. These parameters were not measured inside the quartz cylinder 14. There, the emerging flame caused substantial interference in the observed area of cameras. This led to the partial or full light damage of captured photo and video frames. Therefore, it was difficult to process such photos and video recordings.

Results and discussion

Authors defined the integral characteristics of heterogeneous droplet evaporation. They are the values of the ΔR parameter depending on the initial droplet size and the size of inclusions for combustion products of considered flammable liquids (fig. 2).

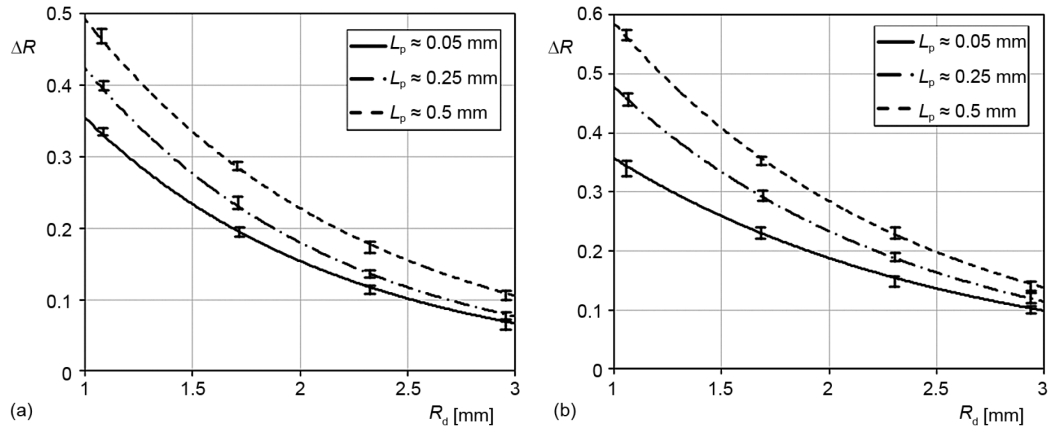

Figure 2. Dependencies $\Delta R = f(R_d)$ by varying L_p at $U_d \approx 2$ m/s, $\gamma_p \approx 0.05$; (a) kerosene, (b) gasoline

For the dependencies depicted in fig. 2(b) (characteristic for gasoline combustion products), we obtained the following approximation equations:

$$\Delta R = 0.6777\exp(-0.641R_d), \quad 1 \le R_d \le 3 \text{ mm}, \quad U_d \approx 2 \text{ m/s}, \quad \gamma_p \approx 0.005, \quad L_p \approx 0.05 \text{ mm} \qquad (1)$$

$$\Delta R = 0.9746\exp(-0.714R_d), \quad 1 \le R_d \le 3 \text{ mm}, \quad U_d \approx 2 \text{ m/s}, \quad \gamma_p \approx 0.005, \quad L_p \approx 0.25 \text{ mm} \qquad (2)$$

$$\Delta R = 1.2073\exp(-0.722R_d), \quad 1 \le R_d \le 3 \text{ mm}, \quad U_d \approx 2 \text{ m/s}, \quad \gamma_p \approx 0.005, \quad L_p \approx 0.5 \text{ mm} \qquad (3)$$

Approximation equations for predicting the integral characteristics of droplet evaporation in the combustion products of other considered flammable liquids have a similar appearance. As a result of summarizing the group of considered combustion products, it is possible to indicate the limits of changing ΔR parameter (fig. 3). There, the values of the ΔR parameter are within the outlined area, when the sizes of inclusions varied from 0.05 to 0.5 mm.

It can be seen that the values of the ΔR parameter may significantly differ by almost several times (under identical initial conditions) for the combustion products of considered flammable liquids widely used in gas-vapor-droplet heat technologies [1-5]. This result illustrates the possibilities of varying the initial parameters (the sizes of droplets, the concentration and size of inclusions, the type of a flammable liquid, the temperature of combustion products) over a wide range for setting up the equipment in technological cycles (in particular, listed in references [1-5]). The dependencies of $\Delta R = f(R_d)$ by varying the concentration of impurities are presented in fig. 4.

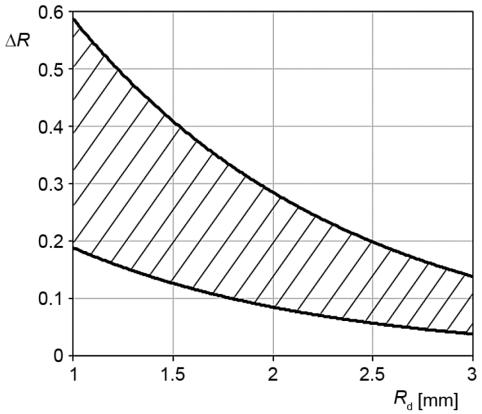

Figure 3. Parameter ΔR for suspension droplets (R_d = 1-3 mm, $\gamma_p \approx 0.005$, L_p = 0.05-0.5 mm) passing the combustion products of considered flammable liquids

For the dependencies depicted in fig. 4(a) (characteristic for gasoline combustion products), we obtained the following approximation equations:

$$\Delta R = 0.6501\exp(-0.922R_d), \quad 1 \le R_d \le 3 \text{ mm}, \quad U_d \approx 2 \text{ m/s}, \quad \gamma_p = 0, \quad L_p \approx 0.05 \text{ mm} \tag{4}$$

$$\Delta R = 0.6777\exp(-0.641R_d), \quad 1 \le R_d \le 3 \text{ mm}, \quad U_d \approx 2 \text{ m/s}, \quad \gamma_p \approx 0.005, \quad L_p \approx 0.05 \text{ mm} \tag{5}$$

$$\Delta R = 0.7907\exp(-0.395R_d), \quad 1 \le R_d \le 3 \text{ mm}, \quad U_d \approx 2 \text{ m/s}, \quad \gamma_p \approx 0.01, \quad L_p \approx 0.05 \text{ mm} \tag{6}$$

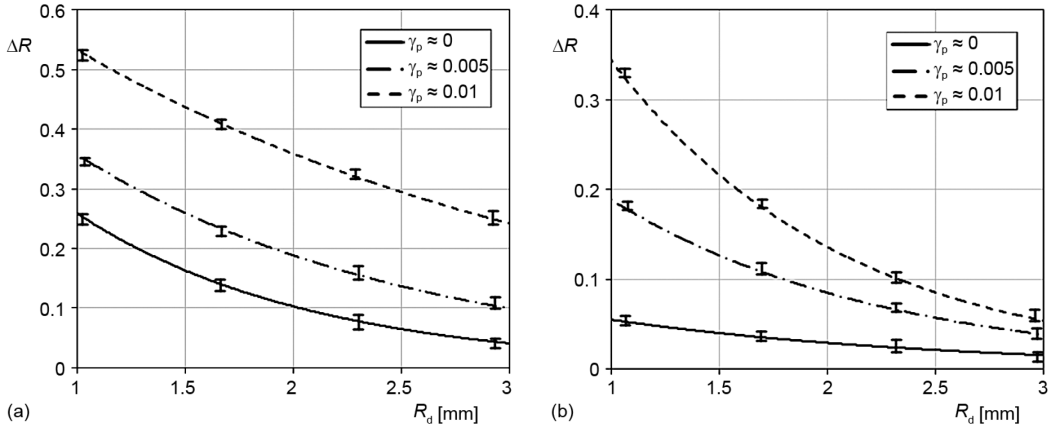

Figure 4. Dependencies $\Delta R = f(R_d)$ by varying γ_p at $U_d \approx 2$ m/s, $\gamma_p \approx 0.05$; (a) – gasoline, (b) – oil

The results summarizing the dependencies of fig. 4 for all considered flammable liquids are presented in fig. 5. Similar to fig. 3, it can be concluded about the difference by several times between the values of the ΔR parameter for the combustion products of all flammable liquids previously discussed.

From the comparison of figs. 4 and 5, we may conclude that the change in the concentration of inclusions (γ_p) leads to the great differences of the ΔR parameter for considered combustion products compared to the sizes of inclusions (L_p). For instance, for droplets with

the initial sizes 2 mm in fig. 3, the ratio of the maximum to the minimum value of ΔR is about 2.5. At $R_d \approx 3$ mm this ratio is about 2.8 (fig. 3). In fig. 4, the ratio is 3-4 for the same initial droplet sizes under identical conditions. This feature can be explained by the great influence of γ_p on heat transfer in a droplet compared to L_p. The changes of ΔR parameter by varying the sizes and concentrations of inclusions are presented in fig. 6.

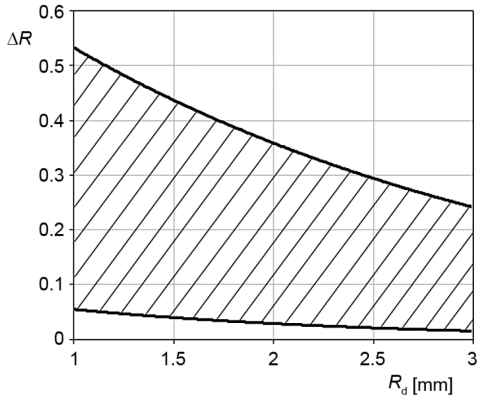

Figure 5. Parameter ΔR for suspension droplets (R_d = 1-3 mm, $L_p \approx$ 0.05 mm, γ_p = 0-0.01) passing the combustion products of considered flammable liquids

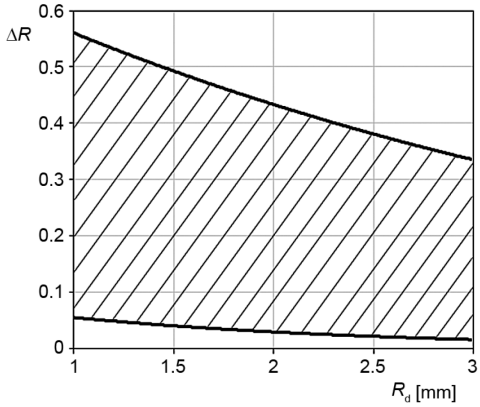

Figure 6. Parameter ΔR for suspension droplets (R_d = 1-3 mm) passing the combustion products of considered flammable liquids (γ_p = 0-0.01 and L_p = 0.05-0.5 mm)

The results of experimental data processing identified several important features. Firstly, in addition to the sizes and concentrations of inclusions, and the initial droplet sizes, droplet velocities U_d have a significant impact on the ΔR values. This is due to the fact that velocities U_d define the lifetime of droplets in high-temperature gas. The experiments demonstrated that the growth of U_d velocities leads to the decrease of ΔR (for example, at $R_d \approx 2$ mm, $\gamma_p \approx 0.005$, $L_p \approx 0.05$ mm, ΔR values are reduced by 15%, while the rate U_d rises from 0.5 m/s to 2 m/s). By increasing γ_p and L_p, the influence of U_d on ΔR strengthens. This result correlates well with the conclusion about the impact of U_d on ΔR for homogeneous water droplets (without additional impurities and inclusions) discussed in the study [11]. Secondly, due to the different scales of the influence of U_d and R_d values to ΔR, it is quite difficult to provide adequate dependencies $\Delta R = f(\mathrm{We_d})$ and $\Delta R = f(\mathrm{Re_d})$. A similar conclusion was made [11] for homogeneous water droplets in preliminary estimates using Weber ($\mathrm{We_d}$) and Reynolds ($\mathrm{Re_d}$) numbers. For their calculation, we took the values of thermophysical characteristics in reference books [19-21]. Third, in all the experiments, the values of Weber numbers for droplets did not exceed limit values ($\mathrm{We_d^{lim}}$ = 8–10), when droplet splitting is possible [22, 23]. At $\mathrm{We_d} < \mathrm{We_d^{lim}}$, it can be excluded from consideration the impact of droplet surface transformation on the integral characteristics of evaporation during the motion in the high-temperature gas.

When analyzing the effect of inclusions from different materials (graphite and aluminum), we established that the conditions of heating up suspension droplets can vary quite significantly. For instance, we revealed that aluminum particles precipitate in droplets despite continuous stirring (due to much greater density than water). This leads to a heterogeneousness of droplet temperature field. In the area with the highest content of inclusions, heat is transferred from the droplet surface to its center more intensively than in the area with a min-

imum content of inclusions. Therefore, it is rather difficult to make an adequate assessment of the intensification of droplet evaporation in general in the experiments with aluminum inclusions. However, we performed relevant assessments for suspension droplets based on water and graphite inclusions. In both cases, such droplets heated up and evaporated more intensively than homogeneous droplets (without additional inclusions and impurities). The main reason for the intensification of heating processes is the increasing role of radiation and conductive heat transfer in a heterogeneous droplet. In this case, the key role is played by not only the factor of thermal conductivity growth of a heterogeneous droplet compared to homogeneous one. Theoretical estimates using models [9, 10] indicate that radiative heat flux to the suspension droplet surface increases by several times under the conditions considered in the experiments. Radiative heat flux to graphite particles, which are in a thin subsurface layer of the heated droplet, is several times higher than the same flow to a water droplet. In studies [9, 10], authors estimated such heat fluxes for carbon and water. It has been shown that for carbon this parameter is 5-6 times greater than for water. Despite the low concentration of inclusions, their temperature may reach much higher values compared to a water droplet. Accordingly, in the vicinity of each inclusion, water heats up and evaporates at a rate that is a multiple greater than the evaporation rate of a homogeneous liquid.

Authors estimated the numerical values of the evaporation rates of a liquid (W_e) in our experiments using the approach as in paper [9]. It has been found that the maximum values of W_e are 0.23-0.34 kg/m^{2}s) for droplets with sizes $1 < R_d < 3$ mm (the maximum size of carbon inclusions was $L_p \approx 0$ .05 mm and their concentration – $\gamma_p \approx 0.01$). In the experiments [9] with homogeneous (without inclusions) water droplets (radius about 3 mm), these values were within a narrower range 0.24-0.27 kg/m^{2}s). The values of W_e for heterogeneous droplets are higher than for homogeneous. At the same time, the range of changing W_e is wider for heterogeneous droplets. This is caused by the relevant difference in the accumulated energy of external gas by inclusions with various sizes and concentrations.

By associating the results of this study and experiments conducted in papers [11, 12], authors compared the values of the ΔR parameter and velocity W_e of a heterogeneous droplet falling through kerosene combustion products at a varying temperature (from 1581 to 572 K) and almost constant temperature T_g (1100 ± 30 K) in the cylinder 14 with a length of 1 m. It has been found that the values of ΔR for droplets with the initial sizes $R_d \approx 3$ mm do not differ by more than 1% under the conditions of non-stationary (T_g decreases from 1581 K to 572 K) and stationary (T_g = 1100 ± 30 K) heating. For droplets with the sizes of about 1 mm, these deviations reach 3-4%. Also, we established the corresponding deviations for evaporation rates W_e. These small deviations for the considered conditions of non-stationary and stationary heating can be explained by inertial heating up and the short times of droplet motion through the channel (less than 0.5 s), as well as a high heat of water vaporization (about 2 MJ/kg). If we calculate the average temperature for the range of 572-1581 K, we obtain 1076.5 K. This value corresponds well to the gas temperature in the experiments [11, 12] at stationary heating conditions (T_g = 1100 ± 30 K). As a consequence, it can be concluded about the possibility of using certain average values of the gas temperature T_g in evaluating or predicting the characteristics of short-term droplet heating (less than 1 seconds). For instance, we can apply prognostic models [9, 10]. The simulation [9, 10] indicated that the heated layer thickness of a water droplet is insufficient for evaporation with the maximum values of W_e for a long period of time (certain energy accumulation is required to be in the droplet, *i. e.* heat flux from the surface to its center). Therefore, the integral characteristics of droplet evapora-

tion in long channels (for example, 5-10 m) differ significantly for non-stationary or stationary heating conditions in high-temperature gases.

Additionally, we conducted experiment with a water droplet containing a single inclusion (on the example of a graphite particle with an average size of 2 mm) to evaluate the influence of the temperature and type of combustion products on the characteristics of heterogeneous droplet evaporation. Droplet sizes (with the inclusion inside the droplet) varied from 2.5 mm to 4 mm. The thickness of the liquid film around the inclusion varied from 0.1 mm to 1 mm. To implement this in practice, a heterogeneous droplet (with a solid inclusion) was put in the cylinder 14 filled with combustion products, with a ceramic rod. We drilled a special technological hole in the inclusion (depth of less than 0.25 mm) to fix it on the ceramic rod. We carried out high-speed video recording of heterogeneous droplet evaporation. For this purpose, we used high-speed cameras 1 and 2 mounted in the upper part of the facility. We determined the times of the complete evaporation of droplets and the laws of their heating up. It has been found out that the vaporization of a liquid droplet with a single large inclusion may occur in one of three modes under the conditions considered in this study. The implementation of each of these modes depends primarily on the gas temperature and the characteristics of inclusion envelopment by a liquid. In the first mode, the conditions of intensive vaporization (boiling and the formation of vapor bubbles) were not reached at the internal borders between the media. The second mode involved the following steps: (1) heating up the liquid film around the inclusion to the conditions of intense vaporization at the internal borders between the media, (2) bubble nucleation was observed on the inclusion surface (usually, after a few seconds from the beginning of heating up the droplet). The third mode corresponded to the conditions of the partial protrusion of the inclusion from the liquid droplet surface. This mode was implemented at gas temperatures over 650 K and was characterized by minimal duration (compared to the other two modes). In the third mode, bubbles were formed at the interface between the media and intensively broke away and merged with neighboring bubbles. When droplet sizes grew rapidly, liquid film thickness multiply decreased. This reduces significantly the liquid pressure relative to vapor pressure inside the droplet. As a result, after the increasing of droplet sizes, we could observe the processes of droplet explosive disintegration, which we may already call typical of the conditions under study, the first experimental results of this process are given in [24]. The times of complete droplet evaporation in the first mode of vaporization (without explosive disintegration) are presented in fig. 7.

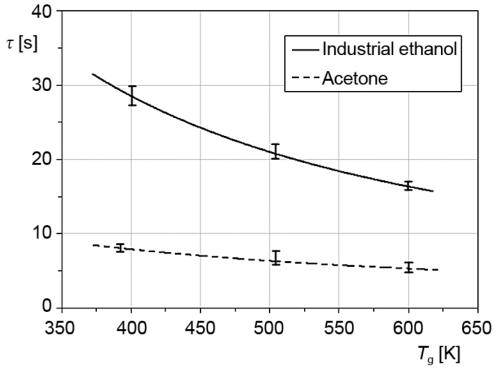

Figure 7. Dependencies of the characteristic times of complete droplet evaporation on the temperature of combustion products for one inclusion ($L_p \approx 2$ mm, $m_p \approx 5$ mg)

The results describe the two types of combustion products, because kerosene, gasoline, and oil are characterized with intense smoke generation. Emerging soot particles were deposited on the droplet surface and hence impeded the monitoring of liquid film thickness, as well as its complete evaporation. It can be seen that the times of liquid complete evaporation are quite significantly different even at comparable temperatures of the combustion products of the flammable liquids under study. It has been found that these differences are reduced with increasing a gas temperature. One can predict that they will be insignificant in the

area of very high gas temperatures. This is because the radiation mechanism of energy supply to the droplet begins to dominate, which leads to the convergence of heating conditions of droplets in the combustion products of considered flammable liquids. The differences between times τ at relatively low gas temperatures (400-600 K) (fig. 7) are due to respective differences between thermophysical properties of combustion products [20-22].

The importance of experimental results for droplets with a single inclusion should particularly emphasized. They not only confirmed the features of the heating and evaporation mechanisms of heterogeneous droplets in basic experiments (figs. 2-6). With their use we could reveal an important effect, which is the possibility of heating up heterogeneous droplets to the conditions of boiling and explosive disintegration (crushing). This effect is important for atomization systems, for example, in firefighting. When releasing several droplets with large inclusions to the combustion zone, we can get tens or even hundreds of much smaller droplets (the area of covering a flame zone by a quenching liquid increases). This will form droplet clouds in the combustion zone. Since the sizes of forming droplets are very small (from tens to hundreds of micrometers), they evaporate rapidly in the flame zone of combustion. As a consequence, in addition to the droplet cloud, a vapor cloud will be formed. Such drip and steam clouds are promising for effective firefighting [3-5]. They reduce the temperature in the combustion zone, displace an oxidant and combustion products by the steam, and prevent the access of an oxidant into the combustion zone from the periphery (*i. e.* they are a buffer layer between the combustion zone and external environment).

Conclusions

We established the integral characteristics of suspension droplet evaporation under the conditions of intensive heating by high-temperature combustion products. Approximation eqs. (1)-(6) and the dependencies $\Delta R = f(R_d)$, $\Delta R = f(L_p)$, and $\Delta R = f(\gamma_p)$ found for the combustion products of typical flammable liquids allowed us to obtain experimental database for the development of the basic elements of the general theory of heterogeneous droplet evaporation under the conditions of the high rates of heating and heat flows. A good correspondence of experimental results (ΔR and W_e values) was obtained for the conditions of non-stationary and almost stationary heating of droplets by high-temperature gases; this allowed us to make conclusions about the possibility of using the average gas temperature in simulating and predicting the characteristics of these processes (during short-term energy supply, typical of modern gas-vapor-droplet high-temperature heat technologies). In the case of prolonged heating (more than 1-2 seconds), the factor of heating rate change plays a decisive role. The experiments with single inclusions identified a number of interesting physical features of heat and mass transfer at the inclusion/liquid interface.

Acknowledgment

The investigations were supported by the Russian Foundation for Basis Research (project 15-38-20006). The studies of the evaporation of water droplets with a single opaque inclusion were supported by the grant of the President of the Russian Federation (project MD-1221.2017.8).

Nomenclature

d_0 – initial droplet diameter, [mm]
d_{01}, d_{02}, d_{03}, d_{04} – maximum sizes (diameters) of single droplets, [mm]
d_1, d_2…d_n – averaged sizes (diameters) of single droplets, [mm]

$d_{drop(px)}$ – conditional average size (diameter) of a single droplet, [px]
$d_{drop(mm)}$ – conditional average size (diameter) of a single droplet, [mm]
$l_{d(px)}$ – distance passed by a droplet in a video frame, [px]
L_p – size of solid inclusions, [mm]
m_d – mass of a suspension droplet, [g]
m_p – mass of solid inclusions in a suspension droplet, [g]
R_d – average size (radius) of a droplet at the input of a high-temperature gas, [mm]
R_d^* – average size (radius) of a droplet at the output from a high-temperature gas, [mm]
Re_d – Reynolds number for droplet, [–]
S – scale factor, [mm per px]
T_g – gas temperature, [K]
T_w – initial water temperature, [K]
t_d – time of droplet motion in a video frame, [s]
$U_{d(px/s)}$ – droplet velocity, [px/s]
U_d – droplet velocity, [m/s]
U_g – gas velocity, [m/s]
W_e – liquid evaporation rate, [$kgm^{-2}s^{-1}$]
ΔR – parameter characterizing the decrease in droplet size during the motion through high-temperature gas, [–]
We_d – Weber number for droplet, [–]
We_d^{lim} – limit value of Weber number for droplet (established in experiments), [–]

Greek symbols

γ_p – mass concentration of solid inclusions in a droplet, [–]
τ – time of droplet evaporation, [s]

References

[1] Terekhov, V. I., *et al.*, Heat and Mass Transfer in Disperse and Porous Media Experimental and Numerical Investigations of Non-Stationary Evaporation of Liquid Droplets, *Journal of Engineering Physics and Thermophysics*, *83* (2010), 5, pp. 883-890
[2] Sazhin, S. S., *et al.*, Multi-Component Droplet Heating and Evaporation: Numerical Simulation versus Experimental Data, *International Journal of Thermal Science*, *50* (2011), 7, pp. 1164-1180
[3] Varaksin, A. Yu., Fluid Dynamics and Thermal Physics of Two Phase Flows: Problems and Achievements, *High Temperature*, *51* (2013), 3, pp. 377-407
[4] Vysokomornaya, O. V., *et al.*, Experimental Investigation of Atomized Water Droplet Initial Parameters Influence on Evaporation Intensity in Flaming Combustion Zone, *Fire Safety Journal*, *70* (2014), Nov., pp. 61-70
[5] Thokchom, A. K., *et al.*, Analysis of Fluid Flow and Particle Transport in Evaporating Droplets Exposed to Infrared Heating, *International Journal of Heat and Mass Transfer*, *68* (2014), Jan., pp. 67-77
[6] Yuen, M. C., Chen, L. W., Heat-Transfer Measurements of Evaporating Liquid Droplets, *International Journal of Heat and Mass Transfer*, *21* (1978), 5, pp. 537-542
[7] Renksizbulut, M., Yuen, M. C., Experimental Study of Droplet Evaporation in a High-Temperature Air Stream, *Journal of Heat Transfer*, *105* (1983), 2, pp. 384-388
[8] Terekhov, V. I., *et al.*, Vortex Pattern of The Turbulent Flow around a Single Cube on a Flat Surface and Its Heat Transfer at Different Attack Angles, *Thermophysics and Aeromechanics*, *17* (2010), 4, pp. 489-500
[9] Kuznetsov, G. V., *et al.*, Estimation of the Numerical Values of the Evaporation Constants of the Water Drops Moving in the High Temperature Gas Flow, *High Temperature*, *53* (2015), 2, pp. 254-258
[10] Glushkov, D. O., *et al.*, Numerical Investigation of Water Droplets Shape Influence on Mathematical Modeling Results of Its Evaporation in Motion through a High-Temperature Gas, *Mathematical Problems in Engineering*, *2014* (2014), ID 920480
[11] Volkov, R. S., *et al.*, Experimental Investigation of Mixtures and Foreign Inclusions in Water Droplets Influence on Integral Characteristics of Their Evaporation during Motion through High-Temperature Gas Area, *International Journal of Thermal Science*, *88* (2015), Feb., pp. 193-200
[12] Glushkov, D. O., *et al.*, Influence of Radiative Heat and Mass Transfer Mechanism in System "Water Droplet-High-Temperature Gases" on Integral Characteristics of Liquid Evaporation, *Thermal Science*, *19* (2015), 5, pp. 1541-1552
[13] Glushkov, D.O., *et al.*, Experimental Investigation of Evaporation Enhancement for Water Droplet Containing Solid Particles in Flaming Combustion Area, *Thermal Science*, 20 (2016), 1, pp. 131-141
[14] Janiszewski, J., Measurement Procedure of Ring Motion with the Use of High Speed Camera during Electromagnetic Expansion, *Metrology and Measurement Systems*, *19* (2012), 2, pp. 797-804
[15] Dehaeck, S., *et al.*, Laser Marked Shadowgraphy: A Novel Optical Planar Technique for the Study of Microbubbles and Droplets, *Experiments in Fluids*, *47* (2009), 2, pp. 333-341

[16] Damaschke, N., *et al.*, Optical Limits of Particle Concentration for Multi-Dimensional Particle Sizing Techniques in Fluid Mechanics, *Experiments in Fluids*, *32* (2002), 2, pp. 143-152
[17] Hadad, T., Gurka, R., Effects of Particle Size, Concentration and Surface Coating on Turbulent Flow Properties Obtained Using PIV/PTV, *Experimental Thermal and Fluid Science*, *45* (2013), Feb., pp. 203-212
[18] Keane, R. D., Adrian, R. J., Theory of Cross-Correlation Analysis of PIV Images, *Applied Scientific Research*, *49* (1992), 3, pp. 191-215
[19] Kothandaraman, C., Subramanyan, S., *Heat and Mass Transfer Data Book*, Halsted Press/Wiley, Hoboken, New York, USA, 1975
[20] Wong, H. Y., *Handbook of Essential Formulae and Data on Heat Transfer for Engineers*, Longman Group, London, 1977
[21] Vargaftik, N. B., *et al.*, *Handbook of Thermal Conductivity of Liquids and Gases*, CRC Press, Boca Raton, Fla., USA, 1994
[22] Wierzba, A., Deformation and Breakup of Liquid Drops in a Gas Stream at Nearby Critical Weber Numbers, *Experiments in Fluids*, *9* (1990), 1, pp. 59-64
[23] Eggers, J., Villermaux, E., Physics of Liquid Jets, *Reports on Progress in Physics*, *71* (2008), ID 036601
[24] Anufriev, I. S., *et al.*, Conditions of Explosive Evaporation at the Phase Interface in an Inhomogeneous Droplet, *Technical Physics Letters*, *41* (2015), 8, pp. 810-813

Paper submitted: August 14, 2015
Paper revised: January 12, 2016
Paper accepted: January 20, 2016